FULL PAPER

Dalton
www.rsc.org/dalton

Anion effects in selective bifunctional metal salt extractants based on aza-thioether macrocycles: co-operative cation–anion binding?†

Mark W. Glenny, Alexander J. Blake, Claire Wilson and Martin Schröder *
School of Chemistry, The University of Nottingham, University Park, Nottingham, UK NG7 2RD

Received 22nd October 2002, Accepted 9th January 2003
First published as an Advance Article on the web 23rd April 2003

The binding of AgX salts (X = NO_3^-, BF_4^- and ClO_4^-) to [15]aneS_2ON_2–$(CH_2CONHCONH–^tBu)_2$ (**L**^{1}) has been assessed by ^{1}H NMR spectroscopy. ^{1}H NMR titration studies of AgX with **L**^{1} and related ligands are interpreted in terms of a range of metal–salt binding interactions. Anion binding occurs *via* a switching mechanism whereby co-ordination of a metal cation to **L**^{1} breaks internal hydrogen-bonding to allow anions to bind to the inner urea hydrogen site on the attached pendant arm. No anion binding occurs in the absence of a bound metal ion. Crystal structures of two complexes **L**·$AgNO_3$ confirm this feature [for N–H ··· ONO_2, N ··· O = 2.866(5)–2.940(5) Å in **L**^{1}·$AgNO_3$], but also show chelate binding of the amide O-donor of the acylurea pendant arm to Ag^I in the solid state. Two-phase metal extraction studies with AgX salts and **L**^{1} confirm that the anion plays an important role, although it is likely that solubility of the resulting metal complexes in the organic phase is the predominant factor. A range of related amide substituted macrocycles has also been prepared and anion binding interactions appear strongest with those ligands containing the highest number of amide/urea units. At high anion concentrations, and in the presence of Ag^I, all of the ligands participate in anion–ligand interactions.

Introduction

Crown thioethers are now a well studied class of ligands with a large body of associated work in the literature.[1] Their co-ordination chemistry is diverse and results in many stable transition metal complexes[2] with unusual co-ordination geometries and/or oxidation states for the metal centres.[1,3] Their ability to behave as selective metal extraction agents for 'soft' metal ions such as mercury[4] has also been reported. In contrast to pure thioether macrocycles, the chemistry of aza-thioether macrocycles has been relatively neglected, although the parent macrocycles [9]aneNS_2,[5] [15]aneNS_4,[6] [12]aneN_2S_2[7] and several other mixed-donor macrocycles[8] have been reported. In addition, a number of *N*-aryl substituted aza-thioether macrocycles are known, some of which demonstrate selective Ag^I extraction and transport.[9] Incorporation of a secondary amine group directly into the thioether macrocyclic ring allows facile functionalisation and this is where our interest in these molecules originates. Combining the ability of thioether macrocycles to co-ordinate 'soft' metal ions, even under acidic conditions, with anion binding sites allows the potential preparation of bifunctional molecules for the binding and extraction of metal salts. We have therefore targeted the synthesis of functional heteroditopic molecules which can co-ordinate both the cation and anion(s) of a metal salt and act as an ion-pair receptor. A few species of this type already exist[10] and may show co-operative ion-pair binding where the complexation of the cation acts as a switch for selective anion co-ordination.[11] It is not uncommon for these types of systems to utilise the well established co-ordinative ability of hosts such as crown ethers and calixarenes combined with anion receptors such as Schiff-base supported uranyls,[12] amides,[1b,2,13] boryls[14] and zinc porphyrins.[15] These compounds are generally only useful for the tandem complexation of Group 1 halides and hydrogen phosphates and are not applicable to the extraction of transition metal salts. However, Tasker and co-workers have recently reported[16] the use of zwitterionic salen-type ligands for binding transition metal salts.

We have already demonstrated that our component-based system, which contains both an aza-thioether macrocyclic unit and an acylurea unit for metal and anion co-ordination, respectively, is effective for binding metal salts in the solid state.[17] The structure of $AgNO_3$·[12]aneS_3N–$CH_2C(O)NHC(O)NH–^tBu$ clearly shows the Ag^I ion co-ordinated inside the [12]aneNS_3 cavity and the NO_3^- anion interacting with the amide functionality on the pendant arm. One of the problems with molecules of this type, designed to interact with substrates *via* hydrogen-bonding, is that there exists an inherent tendency to form intramolecular hydrogen-bonds. This has been noted in particular with other systems containing urea functionalities[10c,18] and is apparent in the systems described here. Interactions of this type must be overcome if a heteroditopic host is to function as an ion-pair receptor where intermolecular hydrogen-bonding to anions is a key function. We report herein structural examples of $AgNO_3$·receptor complexes and seek to address some of the issues surrounding the action of the receptors in solution.

Results and discussion

Aza-thioether host ligands, **L**^{1}–**L**^{10} (Fig. 1), were prepared by reaction of the parent macrocycles with pre-formed anion binding units, *e.g.* 1-*tert*-butyl-3-(chloroacetyl)urea, *N*-*tert*-butyl-2-chloroacetamide and *N*-phenyl-2-chloroacetamide (Fig. 2). The resulting heteroditopic ligands were complexed with AgX salts (X = NO_3^-, BF_4^- and ClO_4^-) and characterised by NMR and infrared spectroscopy, mass spectrometry, elemental analysis and, in some cases, by single crystal X-ray diffraction.

The $AgNO_3$ complex of the acylurea derivatised macrocycle [15]aneS_2ON_2–$(CH_2CONHCONH–^tBu)_2$ (**L**^{1}) was obtained by reaction of the macrocycle with $AgNO_3$ in MeCN solution. Analytical data indicated that the 1:1 complex, **L**^{1}·$AgNO_3$, had been isolated and ^{1}H NMR titration of **L**^{1} with $AgNO_3$ (between 0.125 and 0.875 mol fraction of silver nitrate) confirmed the formation of a 1:1 complex in deuterated MeCN solution.[19] The signals for the macrocyclic methylene hydrogens adjacent to sulfur atoms are observed to shift downfield in the ^{1}H NMR spectrum of the complex (d^3-MeCN) by 0.1 ppm with respect to the free ligand, while the pendant arm methylene hydrogen signal is shifted downfield by 0.32 ppm. While these shifts are indicative of metal ion binding to the macrocycle, our main interest was centred on the urea functionality and whether the NO_3^- anion interacts to any degree with the urea hydrogens.

† Based on the presentation given at Dalton Discussion No. 5, 10–12th April 2003, Noordwijkerhout, The Netherlands.

DOI: 10.1039/b210391p

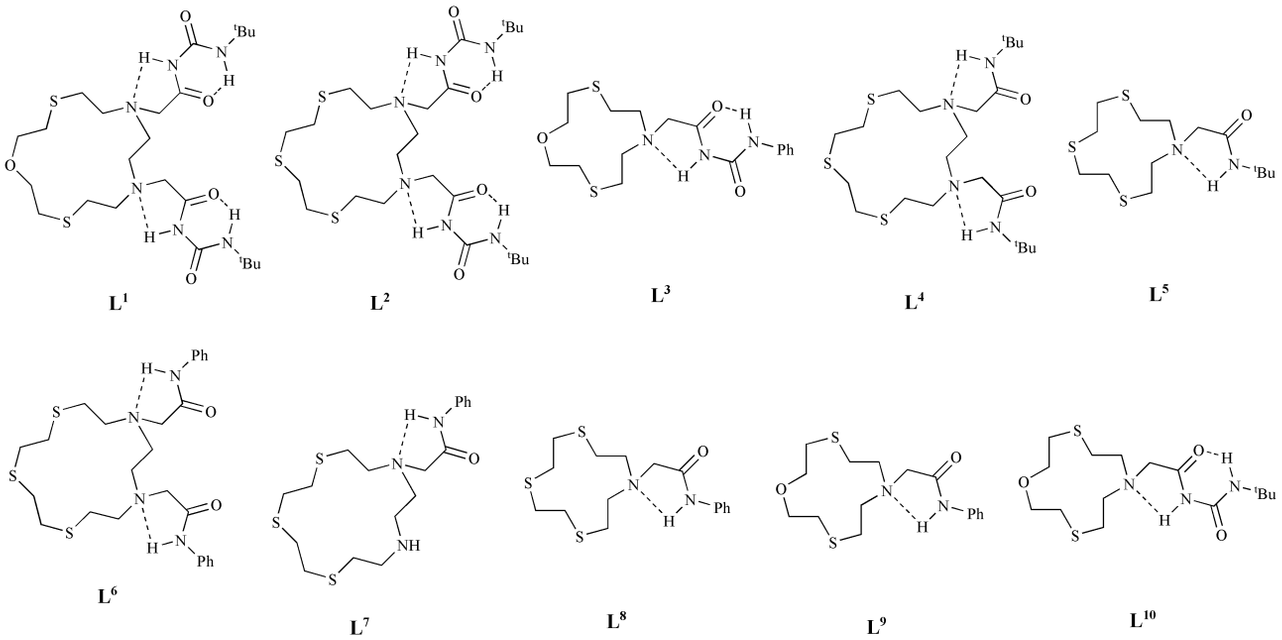

Fig. 1 Structures of ligands $\mathbf{L^1}$–$\mathbf{L^{10}}$.

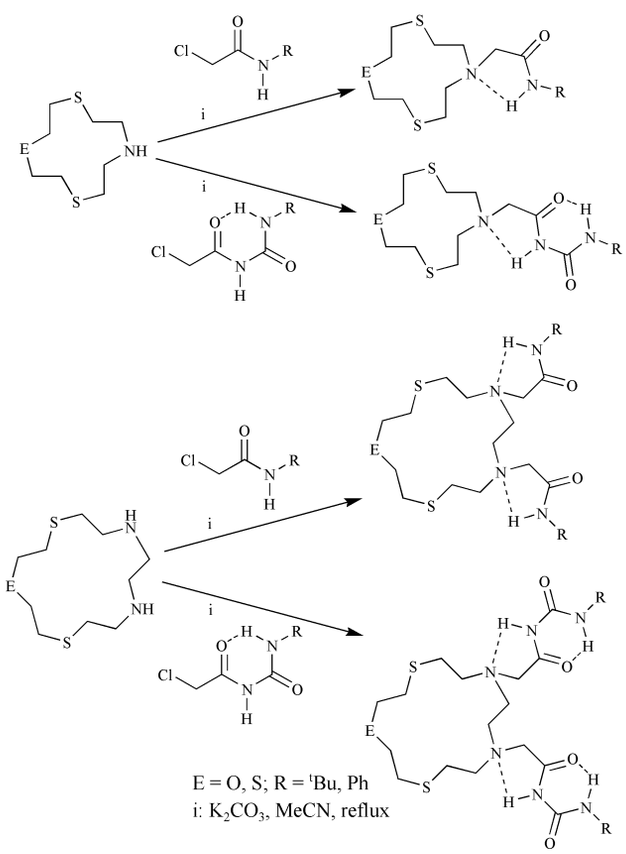

Fig. 2 Synthesis of ligands $\mathbf{L^1}$–$\mathbf{L^{10}}$.

In all of the receptors we have prepared so far, internal hydrogen-bonds are consistently observed between the macrocyclic nitrogen atom and urea or amide hydrogen atoms in the pendant group. In the systems containing acylurea pendant groups, such as $\mathbf{L^1}$, an additional intramolecular hydrogen-bond exists between the outermost urea hydrogen and the acyl oxygen thus holding the urea in a twisted conformation, *i.e.* hydrogens pointing in opposite directions (Fig. 2). A crystal structure of $\mathbf{L^1}$ (Fig. 3) was obtained and clearly shows the presence of both types of hydrogen-bond. In order for anion binding to the urea to occur in $\mathbf{L^1}\cdot AgNO_3$, at least one of the intramolecular hydrogen-bonds must be broken and a new

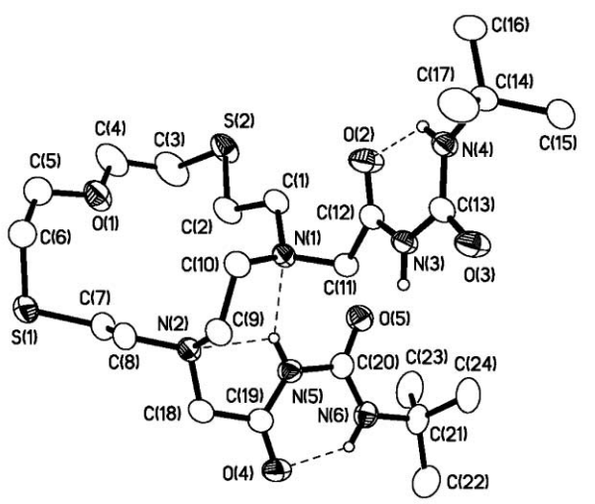

Fig. 3 Crystal structure of $\mathbf{L^1}$ showing the twisted conformation of the pendant arms, intramolecular hydrogen-bonding and *exo* arrangement of the N and S donor atoms. Displacement ellipsoids are drawn at the 50% probability level.

hydrogen-bond to the NO_3^- anion formed. It is usual for anion–amide/urea interactions to result in a downfield shift of the urea hydrogen signals in ^{1}H NMR spectra,[20] the degree of shift indicating the strength of the interaction. The ^{1}H NMR spectrum of $\mathbf{L^1}\cdot AgNO_3$ in d^3-MeCN shows that one of the acylurea hydrogen signals is shifted downfield by 0.33 ppm with respect to the free ligand while the other urea hydrogen signal is shifted upfield by 0.20 ppm. The observation of a downfield shift is consistent with an anion–urea interaction; however, the magnitude of the shift indicates that the interaction may be a weak one, while the upfield shift of the other urea hydrogen signal indicates weakening or breaking of an existing hydrogen-bond.

Owing to the *exo* arrangement of the donor atoms in $\mathbf{L^1}$ (Fig. 3), reorganisation of the donors to an *endo* conformation is necessary to accommodate a metal cation. If, as is likely, the macrocyclic N-donors bind the metal ion the hydrogen-bonds to the urea moieties which are present in the free ligand will be broken upon coordination. This then is the necessary mechanism whereby the previously unavailable inner urea hydrogens are released to interact with anions in solution (Fig. 4). This is

Table 1 ^{1}H NMR chemical shifts (ppm) of $\mathbf{L^1}$·AgX complexes (d^3-MeCN)

Entry	Experiment	NH_{inner}	NH_{outer}	C$H_{2\ pendant}$
1	$\mathbf{L^1}$	9.09	8.22	3.21
2	$\mathbf{L_1}$ + $AgBF_4$	8.26	7.99	3.34
3	$\mathbf{L_1}$ + $AgClO_4$	8.41	8.00	3.37
4	$\mathbf{L^1}$ + $AgNO_3$	9.42	8.02	3.53
5	$\mathbf{L^1}$ + n-Bu_4NO_3	9.09	8.22	3.21
6	$\mathbf{L^1}$ + n-Bu_4N(Ar)[a]	9.52	8.38	3.25
7	$\mathbf{L^1}$ + $AgNO_3$ + 3 equiv. n-Bu_4BF_4	8.56	8.02	3.39
8	$\mathbf{L^1}$ + $AgNO_3$ + 8 equiv. n-Bu_4BF_4	8.51	8.02	3.38
9	$\mathbf{L^1}$ + $AgBF_4$ + 1 equiv. n-Bu_4NO_3	8.26	7.99	3.34
10	$\mathbf{L^1}$ + $AgBF_4$ + 3 equiv. n-Bu_4NO_3	8.80	8.04	3.43
11	$\mathbf{L^1}$ + $AgBF_4$ + 13 equiv. n-Bu_4NO_3	9.20	8.12	3.40
12	$\mathbf{L^1}$ + $AgBF_4$ + 2 equiv. $AgNO_3$	8.26	7.99	3.34
13	$\mathbf{L^1}$ + $AgNO_3$ + 2 equiv. $AgBF_4$	8.26	7.99	3.34

[a] Ar = 4-nitrobenzoate.

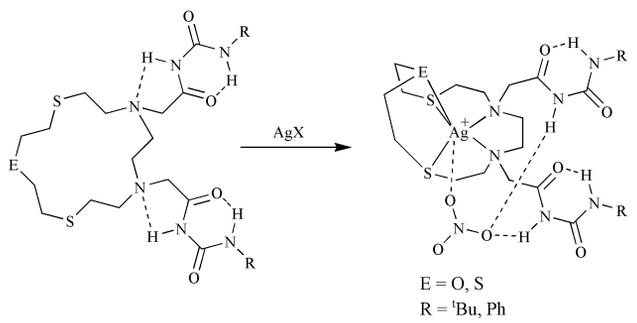

Fig. 4 Proposed rearrangement whereby co-ordination of Ag(I) releases previously unavailable urea hydrogens for hydrogen-bonding to anions.

consistent with the downfield shift observed in the NMR spectrum of $\mathbf{L^1}$·$AgNO_3$. Although this mechanism does not explain the upfield shift of the remaining outer urea signal, the fact that only one urea hydrogen appears to be involved in an interaction is consistent with the twisted conformation observed in the solid state of the free ligand being maintained in solution.

To elucidate the solution dynamics of the system, ^{1}H NMR titration experiments with $AgBF_4$, $AgClO_4$, n-Bu_4NNO_3, n-Bu_4NBF_4 and n-Bu_4N(4-nitrobenzoate) in deuterated MeCN were conducted. Addition of n-Bu_4NNO_3 (10-fold excess) to $\mathbf{L^1}$ afforded no shift of the urea hydrogens, whereas addition of one equivalent of n-Bu_4N(4-nitrobenzoate)[21] produced significant downfield shifts (0.43 and 0.16 ppm, respectively, for the inner and outer hydrogens). The observation of downfield shifts for both urea hydrogens in the latter experiment indicates that the twisted conformation of the pendant group can be altered by the presence of a strongly binding substrate. Importantly, however, no hydrogen-bonds appear to be broken or formed upon addition of NO_3^- to $\mathbf{L^1}$. This is in accord with the mechanism requiring metal-induced reorganisation of the macrocycle to release the inner urea hydrogens and allow anion binding to occur. Hence, this system involves an ion-switch resulting in co-operative binding of the metal salt. There also appears to be very little aggregation of the molecules in MeCN solution, the only shift observed in the ^{1}H NMR spectrum of $\mathbf{L^1}$ upon 100-fold dilution being a downfield shift of 0.06 ppm for the inner urea hydrogens. This represents further evidence that the twisted structure of the free receptor incorporating strong intramolecular hydrogen-bonding is maintained in solution.

Addition of one equivalent of $AgBF_4$ to $\mathbf{L^1}$ results in both urea hydrogen signals shifting upfield (0.83 and 0.23 ppm respectively for the inner and outer hydrogens), whereas addition of an 8-fold excess has no further major effect on the observed chemical shift. Assuming negligible urea–BF_4^- interactions, the direction and magnitude of shift of the inner urea hydrogens in the complex $\mathbf{L^1}$·$AgBF_4$ can be understood on the basis of the reorganisation mechanism involving binding of Ag^I and disruption of internal hydrogen-bonding. This then allows us to use the chemical shift of the inner urea hydrogens in the $\mathbf{L^1}$·$AgBF_4$ complex as a base value to compare the relative strengths of other anion interactions with the receptor. Upfield shifts of 0.68 and 0.22 ppm for the inner and outer hydrogens, respectively, were also observed upon addition of $AgClO_4$ to $\mathbf{L^1}$. However, the shift for the inner urea hydrogen is less than that observed in the presence of $AgBF_4$, indicating that a weak interaction may exist between ClO_4^- and the inner urea hydrogens. Examination of the chemical shift data (Table 1) of the outer urea hydrogen in all three complexes $\mathbf{L^1}$·AgX (X = BF_4^-, ClO_4^- and NO_3^-) shows that it is almost invariant in the presence of different anions, δ 8.00 ± 0.02. This is clear evidence that this outer hydrogen is taking very little part in interactions with the anions.

With this evidence in mind it would appear that the downfield shift of the inner urea hydrogens observed in $\mathbf{L^1}$·$AgNO_3$ indicates that NO_3^- is bound much more strongly than ClO_4^-. It should, therefore, be possible to carry out titration experiments to determine anion binding constants by firstly preparing the complex $\mathbf{L^1}$·$AgBF_4$ and titrating this with tetraalkylammonium salts of the anions of interest. Preliminary experiments carried out to test this using $\mathbf{L^1}$·$AgBF_4$ resulted in downfield shifts of the inner urea hydrogen signal on addition of NO_3^-. However, this was complicated by the outcome of analogous experiments carried out by titrating $\mathbf{L^1}$·$AgNO_3$ with n-Bu_4NBF_4, which resulted in upfield shifts of the inner urea hydrogens. Upfield shifts were also observed upon addition of $AgBF_4$ to $\mathbf{L^1}$·$AgNO_3$, whereas no shift was observed when $AgNO_3$ was added to $\mathbf{L^1}$·$AgBF_4$. This suggests that despite the appearance of stronger anion binding in the case of $\mathbf{L^1}$·$AgNO_3$, the complex $\mathbf{L^1}$·$AgBF_4$ appears to be more stable under certain conditions. It is not easy to interpret these results in a simple manner because of the various competing equilibria occurring in solution, although by careful choice of metal salt and the use of certain assumptions the results become more meaningful. Fig. 5 shows the various equilibria involved in ion-pair binding for a neutral ligand with a Ag^I salt in non-aqueous solvents. If the metal salt is soluble in the solvent used then K_1 can be ignored. Likewise, if the metal is assumed to be always bound to the receptor, which is highly likely given the high selectivity of thioethers for Ag^I, then K_2, K_3, K_4 and K_6 can all be ignored. This leaves only K_5, which we are interested in and would like to measure, and ion-pairing as the major equilibrium processes in solution.

Further examination of the higher field region of the ^{1}H NMR spectrum where the macrocyclic methylene signals occur provides further insight into the differences in binding of the different anions. Two distinct patterns are observed for the macrocyclic methylene hydrogens: one is common to both $\mathbf{L^1}$·$AgBF_4$ and $\mathbf{L^1}$·$AgClO_4$, and the other is observed for $\mathbf{L^1}$·

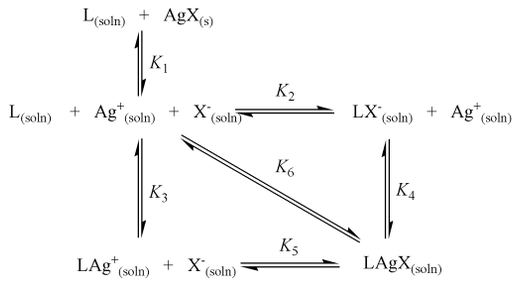

Fig. 5 Equilibria involved in silver salt ion-pair binding with neutral ligands.

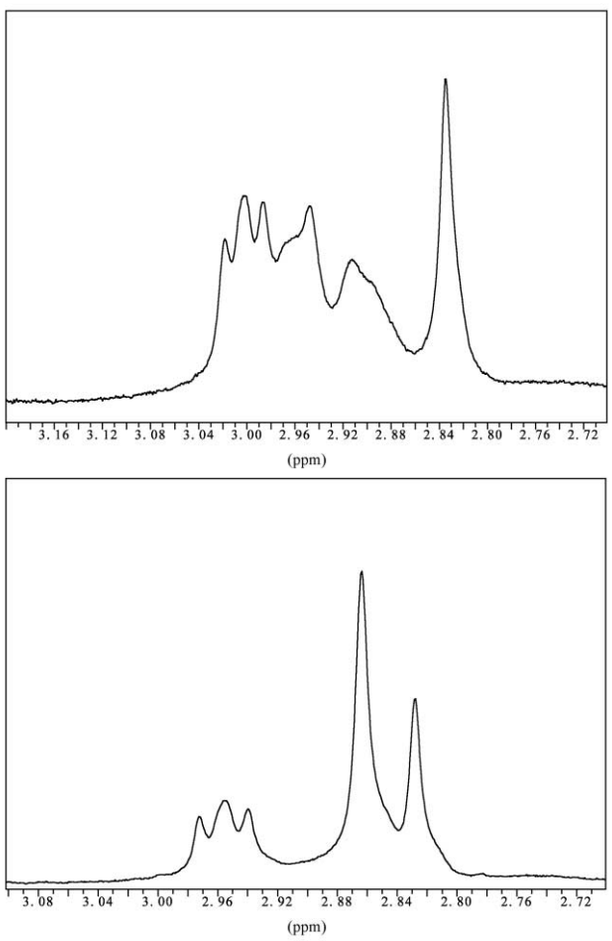

Fig. 6 Macrocyclic methylene resonances in the ^{1}H NMR spectra of $\mathbf{L^1}\cdot AgNO_3$ (top) and $\mathbf{L^1}\cdot AgBF_4$ (bottom).

$AgNO_3$ (Fig. 6). In addition, the signal attributed to the pendant arm methylene units of the $\mathbf{L^1}\cdot AgNO_3$ complex is shifted considerably downfield compared with the BF_4^- and ClO_4^- complexes. Both of these observations are consistent with the co-ordination about Ag^I and/or the conformation of the ligand being different in the presence of different anions. There are several types of interaction that an anion may have with a heteroditopic ligand such as $\mathbf{L^1}$, and these are shown schematically in Fig. 7 with **D** representing little or no interaction of the anion with the complex cation. On the basis of the previous discussion and of the changes in chemical shift upon titration of the complexes with anions, we believe that the complex $\mathbf{L^1}\cdot AgNO_3$ is best represented by **A** or **B**, whereas $\mathbf{L^1}\cdot AgClO_4$ is compatible with **B** or **C**. We assign **D** as a default structure to $\mathbf{L^1}\cdot AgBF_4$. Obviously these are the extreme situations in solution and two or more of these structures may be in equilibrium, yet this proposal does offer an explanation to the previously puzzling order in stability of the complexes. On purely entropic grounds, release of the NO_3^- anion upon the introduction of

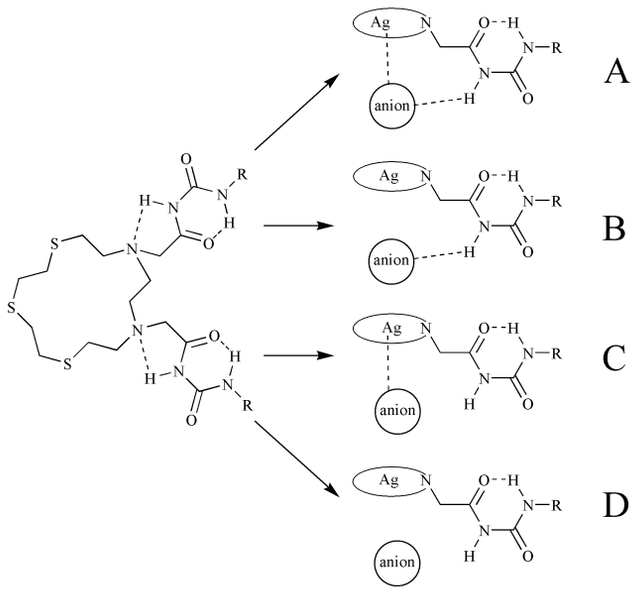

Fig. 7 Proposed anion interactions with acylurea substituted macrocycles (single pendant arm and condensed view of macrocycle shown for simplicity).

competing anions, which must be accompanied by some type of reorganisation, will be favourable if the overall entropy of the system is increased [eqns. (1) and (2)].

$$\mathbf{L^1}\cdot AgNO_3 + xs\,Ag^+ + xs\,BF_4^- \longrightarrow \mathbf{L^1}\cdot Ag^+ + xs\,BF_4^- + xs\,Ag^+ + NO_3^- \quad (1)$$

$$\mathbf{L^1}\cdot AgNO_3 + xs\,n\text{-}Bu_4N^+ + xs\,BF_4^- \longrightarrow \mathbf{L^1}\cdot Ag^+ + xs\,BF_4^- + xs\,n\text{-}Bu_4N^+ + NO_3^- \quad (2)$$

While the mechanism for this type of rearrangement is not obvious, the driving force may be related to the amount of ion-pairing between the various species in solution. Previous studies have shown that in polar aprotic solvents, $AgNO_3$ is more highly ion-paired than $AgBF_4$; and likewise, for the tetraalkylammonium salts, NO_3^- salts appear to be more highly ion-paired.[22] Thus, release of NO_3^- on addition of anions to $\mathbf{L^1}\cdot AgNO_3$ may reflect the greater ion-pairing of NO_3^- salts. However, without calorimetric measurements the entropic and enthalpic contributions are difficult to establish.

The exact structure of $\mathbf{L^1}\cdot AgNO_3$ in solution is difficult to ascertain due to the number of possible donors. Thus, macrocyclic N-, O- and S-donors, acyl O-, urea H-centres, anion and solvent may all play a role. Fortunately, a single crystal of $\mathbf{L^1}\cdot AgNO_3$ suitable for X-ray diffraction was obtained by slow diffusion of Et_2O into a solution of the complex in MeCN. Based on the solution NMR data, we might have expected to observe an interaction between a NO_3^- anion and the Ag^I and urea centres. This, however, is not observed yet the infrared spectrum of the compound displays a peak at 1384 cm^{-1} (νNO) which is unshifted from that of $AgNO_3$ (KBr disc).

The crystal structure of $\mathbf{L^1}\cdot AgNO_3$ shows the asymmetric unit (Fig. 8) to consist of two independent complexes linked through two Ag–S bonds [Ag(1)–S(1) and Ag(2)–S(4); 3.1453(17) and 2.7343(15) Å, respectively (see Table 2)]. There is a hydrogen-bond between a urea hydrogen on one complex unit and a macrocyclic oxygen on the other [for N(5)–H(5A) ··· O(6), N ··· O = 2.867(5) Å]. The structural core is shown in Fig. 9. All outer urea hydrogens are involved in intramolecular hydrogen-bonding to the acyl oxygen of the same pendant arm, while the inner urea hydrogens, except H(5A) which is involved in intermolecular bonding, interact with NO_3^- oxygen atoms [for N(3)–H(3A) ··· O(1A), N(9)–H(9C) ··· O(5A) and N(11)–H(11A) ··· O(6A), N ··· O 2.867(5), 2.940(5) and 2.866(5) Å, respectively]. This is consist-

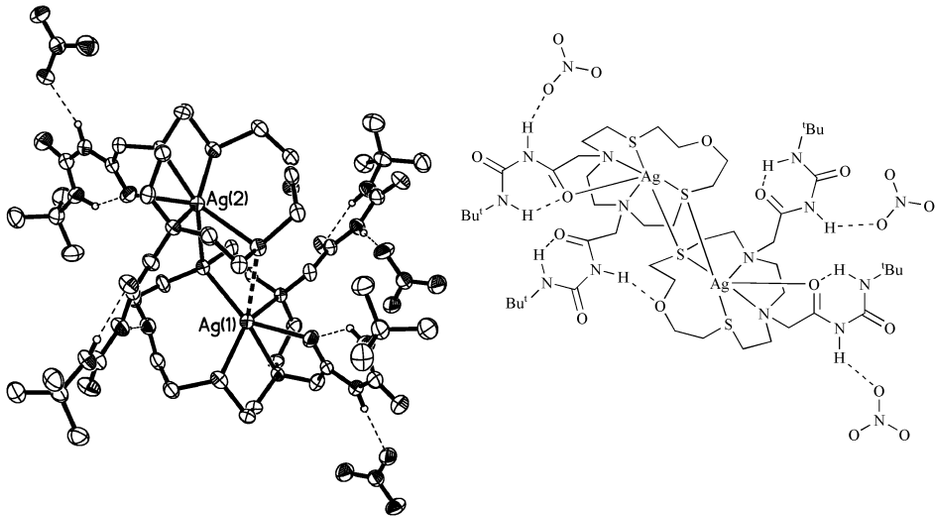

Fig. 8 Crystal structure of $\mathbf{L^1}\cdot AgNO_3$ showing hydrogen-bonding between urea hydrogens and nitrate anions and intramolecular hydrogen-bonds. All non-urea hydrogens have been omitted for clarity and displacement ellipsoids are shown at the 50% probability level.

Table 2 Selected bond lengths (Å), angles (°) for $\mathbf{L^1}\cdot AgNO_3$

Ag(1)–N(7)	2.610(3)	Ag(2)–N(1)	2.454(3)
Ag(1)–N(8)	2.495(3)	Ag(2)–N(2)	2.555(4)
Ag(1)–O(9)	2.505(3)	Ag(2)–S(1)	2.7069(14)
Ag(1)–S(1)	3.1453(17)	Ag(2)–S(2)	2.6700(14)
Ag(1)–S(3)	2.6014(14)	Ag(2)–S(4)	2.7343(15)
Ag(1)–S(4)	2.5495(13)	Ag(2)–O(2)	2.708(3)
N(7)–Ag(1)–N(8)	71.19(11)	N(1)–Ag(2)–N(2)	73.94(12)
N(7)–Ag(1)–O(9)	90.57(10)	N(1)–Ag(2)–O(2)	67.62(11)
N(7)–Ag(1)–S(1)	97.06(9)	N(1)–Ag(2)–S(1)	132.70(9)
N(7)–Ag(1)–S(3)	151.25(8)	N(1)–Ag(2)–S(2)	79.63(9)
N(7)–Ag(1)–S(4)	79.83(8)	N(1)–Ag(2)–S(4)	152.42(9)
N(8)–Ag(1)–O(9)	68.74(11)	N(2)–Ag(2)–O(2)	98.70(11)
N(8)–Ag(1)–S(1)	146.71(9)	N(2)–Ag(2)–S(1)	76.56(8)
N(8)–Ag(1)–S(3)	80.87(8)	N(2)–Ag(2)–S(2)	151.98(8)
N(8)–Ag(1)–S(4)	136.28(8)	N(2)–Ag(2)–S(4)	106.30(9)
O(9)–Ag(1)–S(1)	80.69(8)	O(2)–Ag(2)–S(1)	153.90(7)
O(9)–Ag(1)–S(3)	85.43(8)	O(2)–Ag(2)–S(2)	79.29(8)
O(9)–Ag(1)–S(4)	144.79(8)	O(2)–Ag(2)–S(4)	85.37(8)
S(1)–Ag(1)–S(4)	67.21(4)	S(1)–Ag(2)–S(2)	116.85(4)
S(1)–Ag(1)–S(3)	110.29(5)	S(1)–Ag(2)–S(4)	71.80(4)
S(3)–Ag(1)–S(4)	118.36(4)	S(2)–Ag(2)–S(4)	101.40(5)
Ag(1)–S(1)–Ag(2)	101.32(5)	Ag(1)–S(4)–Ag(2)	118.20(5)

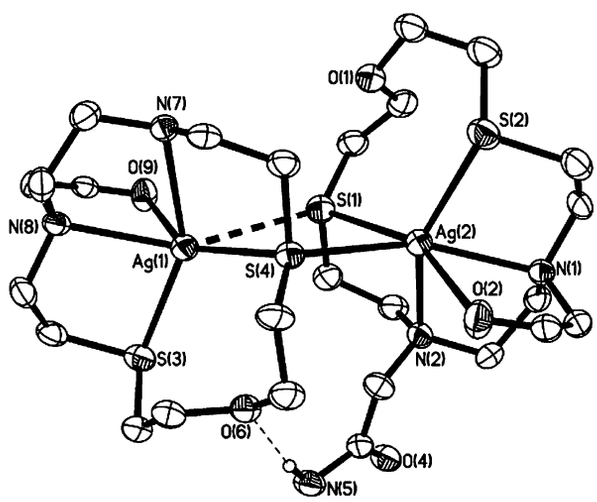

Fig. 9 Crystal structure of $\mathbf{L^1}\cdot AgNO_3$ showing the central core. Hydrogen-bonding of H(5A) to the adjacent macrocyclic oxygen and the long Ag(1)–S(1) interaction are clearly visible. All non-urea hydrogens have been omitted for clarity and displacement ellipsoids are shown at the 50% probability level.

ent with the solution NMR data where only the inner urea hydrogens take part in anion binding. Both complex units are six co-ordinate with severely distorted octahedral geometries about Ag^I, which is bound to both macrocyclic N-donors and three S-donors, two of which are bridging. Significantly, an acyl O-donor from two separate acylurea pendant arms binds to a single Ag^I centre with the remaining two acyl O-donors involved in intramolecular hydrogen-bonding to the outer urea hydrogens within the pendant unit. The observed upfield shift for the outer hydrogens by NMR spectroscopy in solution upon complexation is therefore consistent with carbonyl binding to the encapsulated Ag^I ion and concomitant weakening of the internal hydrogen-bonds at the outer urea centres. The macrocyclic ether O-centre is not involved in any close contacts with the Ag^I ions. Co-ordination of carbonyl moieties to Ag^I is fairly common and many structures containing this fragment have been reported[23] with Ag–O bond distances ranging from 2.194 to 2.995 Å,[24] placing the bonds in this structure at the upper end of this range. Binding of the acyl O-donor can therefore be superimposed onto the binding modes suggested in **A**–**D** (Fig. 7), the solid-state structure suggesting that mode B may predominate in solution. The intramolecular Ag–S bond distances range from 2.5495(13) to 2.7069(14) Å and are typical values for thioether crowns,[25] which are also known to form clusters and oligomers with Ag^I in the solid state.[26] A combination of stereochemical flexibility for both the Ag^I ion[25,27] and the macrocyclic ring is most likely responsible for the unusual structure observed in the solid state.

The related macrocycle, [15]aneS_3N_2–($CH_2CONHCONH$–^{t}Bu)$_2$ ($\mathbf{L^2}$), where a sulfur donor replaces the ether oxygen in $\mathbf{L^1}$, produces very similar results to those found for $\mathbf{L^1}$ with all the Ag^I salts used. In all cases the direction and magnitude of shift upon addition of these salts to $\mathbf{L^2}$ in d^3-MeCN parallel that of $\mathbf{L^1}$, indicating that this ligand also functions as a heteroditopic ion-pair receptor for $AgNO_3$ and $AgClO_4$. Presumably, therefore, $AgNO_3$ binds to $\mathbf{L^2}$ in a similar fashion to that proposed for $\mathbf{L^1}\cdot AgNO_3$. $\mathbf{L^2}$ was treated with one equivalent of $AgBF_4$ in deuterated MeCN to give $\mathbf{L^2}\cdot AgBF_4$. Titration of $\mathbf{L^2}\cdot AgBF_4$ with n-Bu_4NNO_3, between 0.125 and 0.875 mole fraction of NO_3^-, produced downfield shifts of the inner urea hydrogens as expected. Preparation of a Job plot[19] showed the NO_3^- complex to be of 1:1 stoichiometry and the binding constant for NO_3^- anion with $\mathbf{L^2}\cdot Ag^+$ was determined as 49 ± 1 M^{-1} by using the program EQNMR.[28] This value is fairly large considering that anion binding is taking place in MeCN, and that there is no preorganisation of the ligand. A highly preorganised macrocyclic anion receptor, containing three thiourea units, has

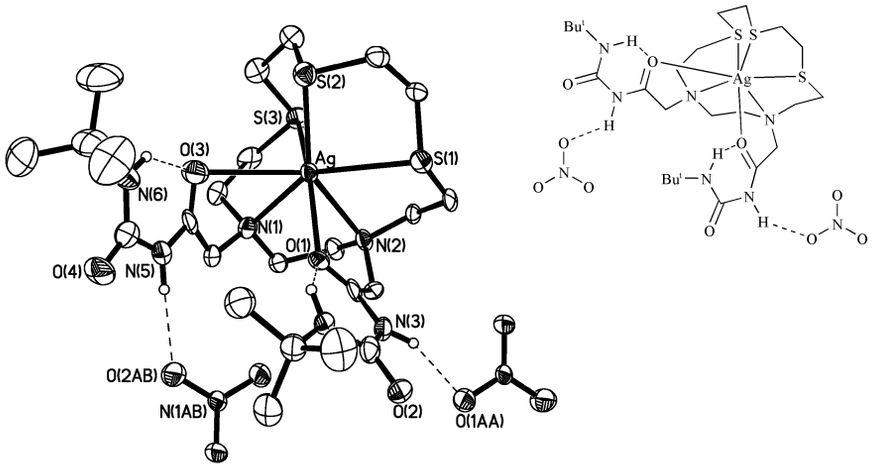

Fig. 10 Crystal structure of $\mathbf{L^2}\cdot AgNO_3$ showing hydrogen-bonding between urea hydrogens and nitrate anions and intramolecular hydrogen-bonds. All non-urea hydrogens have been omitted for clarity and displacement ellipsoids are shown at the 50% probability level.

Table 3 Selected bond lengths (Å), angles (°) for $\mathbf{L^2}\cdot AgNO_3$

Ag–N(1)	2.510(10)	Ag–S(1)	2.928(3)
Ag–N(2)	2.471(10)	Ag–S(2)	2.568(4)
Ag–O(1)	2.600(8)	Ag–S(3)	2.822(4)
Ag–O(3)	2.872(10)		
N(1)–Ag–S(1)	146.5(2)	N(1)–Ag–O(1)	84.6(3)
N(1)–Ag–S(2)	134.4(2)	N(1)–Ag–O(3)	62.3(3)
N(1)–Ag–S(3)	76.3(3)	N(2)–Ag–O(1)	68.8(3)
N(1)–Ag–N(2)	74.2(3)	N(2)–Ag–O(3)	131.5(3)
N(2)–Ag–S(1)	73.3(2)	O(1)–Ag–O(3)	86.3(3)
N(2)–Ag–S(2)	146.7(2)	O(1)–Ag–S(1)	76.5(2)
N(2)–Ag–S(3)	92.4(3)	O(1)–Ag–S(2)	122.0(2)
S(1)–Ag–S(2)	78.95(10)	O(1)–Ag–S(3)	156.3(2)
S(1)–Ag–S(3)	112.70(10)	O(3)–Ag–S(1)	141.5(2)
S(2)–Ag–S(3)	81.60(11)	O(3)–Ag–S(2)	81.7(2)
		O(3)–Ag–S(3)	96.8(2)

a binding constant for NO_3^- of 17.1 ± 0.4 M^{-1} in DMSO,[29] whereas a tweezer-type receptor containing only two (amide) hydrogen-bonding sites has a binding constant for NO_3^- of 27 ± 1.4 M^{-1} in $CHCl_3$.[30]

Reaction of $\mathbf{L^2}$ with $AgNO_3$ in MeCN and subsequent slow diffusion of Et_2O into a solution of the complex afforded small colourless crystals suitable for X-ray diffraction. The crystal structure of $\mathbf{L^2}\cdot AgNO_3$ shows the complex to be monomeric with a seven co-ordinate Ag^I ion (Fig. 10). In $\mathbf{L^2}\cdot AgNO_3$, both acyl oxygen atoms of the pendant arms are found to co-ordinate to the encapsulated metal [Ag–O(1) 2.600(8), Ag–O(3) 2.872(10) Å (see Table 3)], the presence of the additional S-donor in $\mathbf{L^2}$ inhibiting the formation of a dimer *via* bridging sulfur centres in the solid state as observed in $\mathbf{L^1}\cdot AgNO_3$. Potentially vacant co-ordination sites on one side of the metal cation are filled by the acyl O-donors. Given the small but significant upfield shift of the urea hydrogens in the ^1H NMR spectra of both $\mathbf{L^1}\cdot AgNO_3$ and $\mathbf{L^2}\cdot AgNO_3$, it is likely that this Ag–O(acyl) interaction is also present in solution (MeCN), thus weakening the intramolecular hydrogen-bond between this oxygen and the nearby urea hydrogen centres.

Of the three main stereochemistries for seven co-ordinate complexes – pentagonal bipyramidal, capped trigonal prismatic and capped octahedral,[31] all of which are very similar in energy with a variety of intermediate structures available [32] – the complex $\mathbf{L^2}\cdot AgNO_3$ is probably best described as a slightly twisted capped trigonal prism. One trigonal face consists of N(1), O(1) and O(3), the other comprises S(1), S(2) and S(3) with N(2) as the capping atom. Two of the Ag–S bond distances are long [Ag–S(1) and Ag–S(3); 2.928(3) and 2.822(4) Å, respectively] and lie well into the upper quartile of Ag–S distances in thioether complexes.[25] This may be a result of the high co-ordination number of Ag^I in this complex, although the remaining Ag–S(2) distance is more typical at 2.568(4) Å. As found in the structure of $\mathbf{L^1}\cdot AgNO_3$, the inner acylurea hydrogens in $\mathbf{L^2}\cdot AgNO_3$ are involved in hydrogen-bonding interactions with NO_3^- anions of adjacent molecules [for N(3)–H(3C) ··· O(1A) and N(5)–H(5C) ··· O(2A), N ··· O 2.926(14) and 2.917(15) Å, respectively] and the twisted conformation of the pendant arms is also observed. The hydrogen-bonds between urea groups and NO_3^- anions in this complex are also typical for this kind of interaction, with values for other structurally characterised examples usually lying in the range 2.8–3.0 Å.[33] As for $\mathbf{L^1}\cdot AgNO_3$, the NO_3^- stretching mode in the IR spectrum of $\mathbf{L^2}\cdot AgNO_3$ is found at the same position as that in $AgNO_3$ (1384 cm^{-1}).

Comparison of the bifunctionalised macrocycles $\mathbf{L^1}$ and $\mathbf{L^2}$ with related monofunctionalised ligands, containing only one pendant unit, *e.g.* [12]aneS_2ON–CH_2CONHCONH–^{t}Bu ($\mathbf{L^{10}}$, Fig. 1), indicates that anion binding is diminished when the number of urea hydrogens available to bind anions is reduced. A more thorough investigation of related tweezer-type anion receptors has suggested that the degree of NO_3^- binding is highly dependent upon the number of hydrogen-bond donors, with every additional hydrogen-bond adding around 2–3 kJ mol^{-1} to the free energy of complexation.[30] Difficulties in isolating a pure Ag^I complex product were experienced with this particular ligand, which was used only in NMR titration experiments. Substitution of the urea *tert*-butyl end group for a phenyl group, as in [12]aneS_2ON–CH_2CONHCONHPh ($\mathbf{L^3}$), results in the urea hydrogen resonances shifting downfield for the free ligand by more than 1 ppm in the ^1H NMR spectrum due to inductive effects. Addition of $AgNO_3$ to $\mathbf{L^3}$ results in a large upfield shift for the outer urea hydrogen and a smaller shift of the inner hydrogen, although upon addition of excess $AgNO_3$ the inner hydrogen signal begins to shift downfield toward the value found for the free ligand. This suggests that as the anion concentration is increased, anion binding becomes more pronounced. No evidence was found for the presence of $\mathbf{L}\cdot AgNO_3$ ion-pairs in the electrospray mass spectra for any of the complexes.

Since the studies described so far indicated that the outer urea hydrogen centres do not participate in anion binding interactions, ligands were prepared which contain a single amide function in the pendant arm (Fig. 1): [15]aneS_3N_2–(CH_2CONH–^{t}Bu)$_2$ ($\mathbf{L^4}$), [12]aneS_3N–CH_2CONH–^{t}Bu ($\mathbf{L^5}$), [15]aneS_3N_2–(CH_2CONHPh)$_2$ ($\mathbf{L^6}$), [15]aneS_3N_2–CH_2CONHPh ($\mathbf{L^7}$), [12]aneS_3N–CH_2CONHPh ($\mathbf{L^8}$) and [12]aneS_2ON–CH_2CONHPh ($\mathbf{L^9}$). The $AgNO_3$ complexes of all six ligands were prepared in an analogous manner to $\mathbf{L^1}\cdot AgNO_3$ and all showed upfield shifts in their amide hydrogen signals.

However, small downfield shifts were observed with higher **L**:$AgNO_3$ ratios indicating possible anion–amide interactions at high anion concentrations. Aggregation of the ligands does not appear to be significant in MeCN solution since the position and appearance of the signals in the ^{1}H NMR spectrum do not change to any great extent on dilution. The use of IR spectroscopy to identify interactions of NO_3^- with the ligands was not conclusive. This is due in part to the significant changes which occur to the hydrogen-bonding network upon Ag^I co-ordination, but it also appears that the hydrogen-bonding observed in the crystal structure is too weak to have a significant effect on the position of the NO_3^- stretching frequency.

Extraction of silver

Owing to the high affinity of the ligands for Ag^I and the apparent structural changes in the presence of different anions, we were interested in the effect that this may have on the ability of the ligands to extract different Ag^I salts in a two phase aqueous–organic system. Extraction studies were carried out with **L²** and AgX salts (X = NO_3^-, BF_4^- and ClO_4^-) with the apparatus described in the Experimental section which contains an aqueous source phase and an organic receiving phase. After 2 h the Ag^I remaining in the source phase was analysed by AAS and the amount of Ag^I extracted in the presence of different anions expressed as a percentage occupancy of the ligand. Distribution coefficients were not determined from these experiments as the Ag^I concentration was deliberately kept higher than that of the ligand. The results are plotted in Fig. 11.

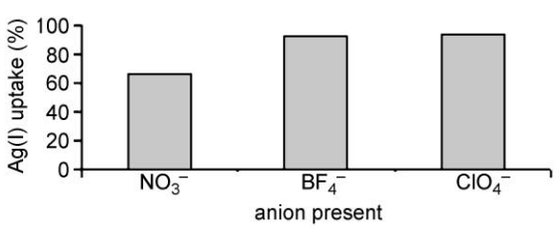

Fig. 11 Graph showing effect of anion on Ag(I) extraction using **L²**.

It can be seen that $AgNO_3$ is extracted least, whereas similar amounts of Ag^I are extracted in the presence of the poorly co-ordinating anions BF_4^- and ClO_4^-. This is in accord with the stabilities of the various complexes in the presence of excess metal salt but, owing to the different solvents used, it is more likely a reflection of the solubility of the metal complexes in the organic phase. The amount of bleeding of metal complex into the aqueous phase was not determined although this should be minimal since the complexes show low solubility in water. Extraction experiments with **L¹** gave similar results and in the presence of acids (HNO_3 or HBF_4) the amount of Ag^I extracted was reduced by less than 10%, reflecting the lack of protonation sites in the ligands which bind metal cations effectively *via* S-donors even at low pH.

Conclusions

A switching mechanism has been identified in these systems whereby a hydrogen-bond between the macrocyclic N-centre and a urea or amide hydrogen is disrupted upon co-ordination of Ag(I) ions and subsequent hydrogen-bonding to anions, *via* the 'free' pendant unit, is then allowed. Such a co-operative effect between cation and anion binding sites is of great interest given the relative simplicity of the ligand design, and shows how systems based on simple components can produce effective results. In the absence of a bound metal ion internal hydrogen-bonding appears to be stronger than intermolecular hydrogen-bonding. It appears that better anion binding can be expected with ligands containing more urea/amide units. This is complicated by solution dynamics where, in the presence of competing anions, new equilibria are established which act to reduce the stability of the metal salt complexes formed. This is especially noticeable with **L¹**·$AgNO_3$ where, despite the apparently large anion binding strength, other factors take precedence in solution to form complexes where anion binding does not play a predominant role in the overall complex stability. Both solution and solid-state structural data are consistent with the inner hydrogen of the acylurea pendant arms contributing to anion binding, while an additional novel binding of the acyl O-donor is confirmed in the solid state. The ligands are highly effective at complexing Ag^I salts as shown by extraction studies, although the effect of different anions on extraction ability is marked and is probably related to the solubility of the resulting metal salt complex in the organic phase.

Experimental

Aza-thioether parent macrocycles were prepared in our laboratory and all other reagents and solvents were purchased from commercial sources and used as received unless stated otherwise. Complexes of $AgNO_3$ were prepared by adding an MeCN solution of $AgNO_3$ to a solution of the appropriate ligand dissolved in MeCN (or an MeCN–CH_2Cl_2 mixture). In a typical procedure $AgNO_3$ (0.2 mmol) in MeCN (2 mL) was added to **L** (0.2 mmol) in MeCN (2 mL) and the mixture heated gently for one minute. Slow diffusion of diethyl ether into the resulting mixture afforded a white precipitate after several days (yield >80%). In some circumstances the product is insoluble in the reaction medium and was isolated by filtration or centrifugation. Diffraction-quality crystals were grown by slow diffusion of diethyl ether into MeCN or methanolic solutions of the complexes.

Metal extraction

The extraction apparatus consisted of vials (30 mL capacity) containing 10 mL of an unbuffered aqueous source phase (AgX and NaX, X = NO_3^-, BF_4^- and ClO_4^-; [Ag^I] = 4.2 mmol L^{-1} with total anion concentration at 50 mmol L^{-1}) and an organic receiving phase (1,2-dichloroethane, 5 mL) containing **L¹** (0.038 mmol). The vials were shaken at 700 rpm (IKA Vibrax-VXR) for 120 min and the source phase analysed by AAS for remaining Ag^I. All values are mean values of duplicate runs.

X-Ray structure analyses

A summary of the crystal data and refinement parameters for **L¹**, **L¹**·$AgNO_3$ and **L²**·$AgNO_3$ is given in Table 4. Data for **L¹**·$AgNO_3$ were collected on an Nonius KappaCCD area detector. Data for **L¹** and **L²**·$AgNO_3$ were collected on a Bruker SMART1000 CCD area detector. Crystals were cooled using Oxford Cryosystems open-flow nitrogen cryostats.[34] Data were corrected for Lorentz and polarisation effects and absorption corrections were also applied. The structures were solved by direct methods[35] and subsequent difference-Fourier syntheses.[36] All non-H atoms, except those in disordered residual ether molecules in **L²**·$AgNO_3$, were refined anisotropically and all H atoms were placed at calculated positions and thereafter refined with $U_{iso}(H) = 1.2U_{eq}(C)$. The structure of **L¹** contains a disordered dichloromethane solvent molecule which was modelled over two sites that were found to be occupied in the ratio 80:20. The crystal of **L²**·$AgNO_3$ decayed suddenly during acquisition and a decay correction was applied. The partially-occupied Et_2O solvent molecule is also disordered and has been modelled over two sites with occupancies 0.3 and 0.2 and the application of geometric restraints.

CCDC reference numbers 195912–195914.

See http://www.rsc.org/suppdata/dt/b2/b210391p/ for crystallographic data in CIF or other electronic format.

Table 4 Crystal data and structure determination details

Compound	$\mathbf{L^1}$	$\mathbf{L^1}\cdot AgNO_3$	$\mathbf{L^2}\cdot AgNO_3$
Formula	$C_{25}H_{48}Cl_2N_6O_5S_2$	$C_{48}H_{92}Ag_2N_{14}O_{16}S_4$	$C_{26}H_{51}AgN_7O_{7.50}S_3$
M	647.71	1465.34	785.79
Crystal system	Triclinic	Triclinic	Triclinic
Space group	$P\bar{1}$	$P\bar{1}$	$P\bar{1}$
a/Å	10.3080(7)	12.8639(3)	9.662(4)
b/Å	10.3129(7)	15.5509(4)	11.141(4)
c/Å	16.9116(11)	17.1342(7)	18.973(7)
α/°	88.351(1)	93.6089(12)	77.451(5)
β/°	84.537(1)	96.4705(12)	79.171(5)
γ/°	72.061(1)	110.9970(16)	82.495(4)
U/Å^3	1702.6(3)	3159.85(17)	1949.4(13)
Z	2	2	2
T/K	150(2)	150(2)	150(2)
μ(Mo-Kα)/mm^{-1}	0.354	0.826	0.725
Reflections collected	17399	46416	8277
Unique reflections, R_{int}	7793, 0.016	14123, 0.125	5968, 0.053
R_1	0.0678 [5620 $I > 2\sigma(I)$]	0.0539 [7759 $I > 2\sigma(I)$]	0.103 [4772 $I > 2\sigma(I)$]
wR_2 (all data)	0.180	0.120	0.271

L^1, [12]aneS$_2$ON$_2$–(CH$_2$CONHCONH–^{t}Bu)$_2$. To a suspension of K_2CO_3 (1.5 g, 10.86 mmol), and KI (0.8 g, 4.82 mmol) in CH_3CN (50 mL) was added [15]aneN$_2$OS$_2$ (0.945 g, 3.78 mmol) and 1-*tert*-butyl-3-(chloroacetyl)urea (1.45 g, 7.55 mmol) and the mixture heated at reflux for 3 h. The solvent was removed and the resulting solid extracted with dichloromethane and washed with water, brine and finally dried over $MgSO_4$. After filtration and evaporation of the solvent, the product was obtained as a white solid (1.49 g, 67%). Recrystallisation from dichloromethane–hexane mixtures, or chromatography (silica gel, dichloromethane–3% methanol eluent) affords a purer product. Anal. calc. for $C_{24}H_{46}N_6O_5S_2$: C, 51.22; H, 8.24; N, 14.93. Found: C, 50.88; H, 8.12; N, 14.52%. ^{1}H NMR ($CDCl_3$): δ (ppm) 1.34 and 1.35 (s, 18H, CMe_3), 2.79 (m, 16H, CH_2), 3.17 (s, 4H, CH_2), 3.70 (m, 4H, CH_2), 8.19 (br, s, 2H, NH), 9.19 (br, s, 2H, NH). ^{13}C NMR ($CDCl_3$): δ (ppm) 28.80 (CMe_3), 30.09 (CH_2), 31.87 (CH_2), 50.70 (CMe_3), 51.99 (CH_2), 55.33 (CH_2), 59.36 (CH_2), 73.00 (CH_2), 151.20 (CO), 172.48 (CO). IR (cm^{-1}) 3289 br (νNH), 1715 (νCO), 1552 (νCO). FAB$^+$-MS m/z ($C_{24}H_{46}N_6O_5S_2$, 562): 563 (M + H$^+$).

L^2, [15]aneS$_3$N$_2$–(CH$_2$CONHCONH–^{t}Bu)$_2$. Using the same procedure as outlined above for the preparation of $\mathbf{L^1}$, [15]aneN$_2$S$_3$ (0.46 g, 1.74 mmol) and 1-*tert*-butyl-3-(chloroacetyl)urea (0.67 g, 3.48 mmol) afforded 0.66 g (66%) of the product as a white solid after chromatography on silica-60 (dichloromethane–methanol, 10:1 eluent) and drying under reduced pressure. Large crystals were obtained by recrystallisation from 1,2-dichloroethane–hexane. Anal. calc. for $C_{24}H_{46}N_6O_4S_3$: C, 49.80; H, 8.01; N, 14.52. Found: C, 49.79; H, 7.99; N, 14.43%. ^{1}H NMR ($CDCl_3$): δ (ppm) 1.36 (s, 18H, CMe_3), 2.81 (m, 20H, CH_2), 3.22 (s, 4H, CH_2), 8.19 (br, s, 2H, NH), 9.29 (br, s, 2H, NH). ^{13}C NMR ($CDCl_3$): δ (ppm) 28.81 (CMe_3), 29.96 (CH_2), 32.54 (CH_2), 32.83 (CH_2), 50.75 (CMe_3), 52.76 (CH_2), 55.36 (CH_2), 58.64 (CH_2), 151.29 (CO), 172.41 (CO). IR (cm^{-1}) 3287, 3232 (νNH), 1712 (νCO), 1550 (νCO). FAB$^+$-MS m/z ($C_{24}H_{46}N_6O_4S_3$, 578): 579 (M + H$^+$).

L^3, [12]aneS$_2$ON–CH$_2$CONHCONHPh. Using the same procedure as outlined above for the preparation of $\mathbf{L^1}$, [12]aneNOS$_2$ (0.268 g, 1.29 mmol) and 1-phenyl-3-(chloroacetyl)urea (0.275 g, 1.29 mmol) afforded 0.66 g (66%) of the product as an orange solid after chromatography on silica-60 (dichloromethane–methanol, 20:1 eluent) and drying under reduced pressure. Anal. calc. for $C_{17}H_{25}N_3O_3S_2$: C, 53.24; H, 6.57; N, 10.96. Found: C, 52.79; H, 6.18; N, 10.61%. ^{1}H NMR ($CDCl_3$): δ (ppm) 2.75 (m, 4H, CH_2), 2.93 (m, 8H, CH_2), 3.32 (s, 2H, CH_2), 3.81 (m, 4H, CH_2), 7.09 (t, 1H, Ph), 7.32 (t, 2H, Ph), 7.53 (d, 2H, Ph), 9.83 (br, s, 1H, NH), 10.35 (br, s, 1H, NH). ^{13}C NMR ($CDCl_3$): δ (ppm) 29.36 (CH_2), 30.85 (CH_2), 52.75 (CH_2), 59.57 (CH_2), 73.98 (CH_2), 120.02 (C_{quat}), 123.96 (CH), 128.78 (CH), 137.18 (C_{quat}), 149.87 (CO), 173.48 (CO). IR (cm^{-1}) 3239 (νNH), 1712 (νCO), 1683 (νCO). FAB$^+$-MS m/z ($C_{17}H_{25}N_3O_3S_2$, 383): 384 (M + H$^+$).

L^4, [15]aneS$_3$N$_2$–(CH$_2$CONH–^{t}Bu)$_2$. Using the same procedure as outlined above for the preparation of $\mathbf{L^1}$, [15]aneN$_2$S$_3$ (0.0763 g, 0.286 mmol) and *N*-*tert*-butyl-2-chloroacetamide (0.086 g, 0.573 mmol) afforded 0.12 g (85%) of the product as a white wax. After chromatography on silica-60 (dichloromethane–methanol, 10:1 eluent) and drying under reduced pressure the product obtained appeared pure by NMR spectroscopy. Anal. calc. for $C_{22}H_{44}N_4O_2S_3$: C, 53.62; H, 9.00; N, 11.37. Found: C, 52.56; H, 8.71; N, 10.09%. ^{1}H NMR ($CDCl_3$): δ (ppm) 1.31 (s, 18H, CMe_3), 2.62–2.80 (m, 20H, CH_2), 2.94 (s, 4H, CH_2), 7.06 (br, s, 2H, NH). ^{13}C NMR ($CDCl_3$): δ (ppm) 28.70 (CMe_3), 30.40 (CH_2), 32.83 (CH_2), 50.67 (CMe_3), 52.28 (CH_2), 54.98 (CH_2), 60.15 (CH_2), 169.50 (CO). FAB$^+$-MS m/z ($C_{22}H_{44}N_4O_2S_3$, 492): 493 (M + H$^+$).

L^5, [12]aneS$_3$N–CH$_2$CONH–^{t}Bu. Using the same procedure as outlined above for the preparation of $\mathbf{L^1}$, [12]aneNS$_3$ (0.0498 g, 0.424 mmol) and *N*-*tert*-butyl-2-chloroacetamide (0.0635 g, 0.424 mmol) afforded 0.13 g (91%) of the product as a white crystalline solid. An analytically pure sample was obtained by recrystallisation from a dichloromethane–hexane mixture. Anal. calc. for $C_{14}H_{28}N_2OS_3$: C, 49.96; H, 8.38; N, 8.32. Found: C, 49.64; H, 8.44; N, 8.33%. ^{1}H NMR ($CDCl_3$): δ (ppm) 1.38 (s, 9H, CMe_3), 2.69 (m, 8H, CH_2), 2.83 (m, 8H, CH_2), 2.96 (s, 2H, CH_2), 7.22 (br, s, 1H, NH). ^{1}H NMR (d^3-MeCN): δ (ppm) 1.35 (s, 9H, CMe_3), 2.67 (s, br, 8H, CH_2), 2.78 (s, br, 8H, CH_2), 2.88 (s, 2H, CH_2), 7.18 (br, s, 1H, NH). ^{13}C NMR ($CDCl_3$): δ (ppm) 27.31 (CH_2), 28.36 (CH_2), 28.72 (CMe_3), 29.50 (CH_2), 50.94 (CMe_3), 53.05 (CH_2), 59.26 (CH_2), 169.36 (CO). IR (cm^{-1}) 3252 (νNH), 3079 (νNH), 1646 (νCO), 1572 (νCO). FAB$^+$-MS m/z ($C_{14}H_{28}N_2OS_3$, 336): 337 (M + H$^+$).

L^6, [15]aneS$_3$N$_2$–(CH$_2$CONHPh)$_2$. Using the same procedure as outlined above for the preparation of $\mathbf{L^1}$, [15]aneN$_2$S$_3$ (0.215 g, 0.807 mmol) and *N*-phenyl-2-chloroacetamide (0.274 g, 1.62 mmol) afforded 0.30 g (70%) of the product as a white solid after washing with acetone and drying under reduced pressure. Anal. calc. for $C_{26}H_{36}N_4O_2S_3$: C, 58.61; H, 6.81; N, 10.52. Found: C, 58.41; H, 6.52; N, 10.35%. ^{1}H NMR ($CDCl_3$): δ (ppm) 2.90 (m, 20H, CH_2), 3.24 (s, 4H, CH_2), 7.10 (t, 2H, Ph), 7.32 (t, 4H, Ph), 7.63 (d, 4H, Ph), 9.29 (br, s, 2H, NH). ^{13}C NMR ($CDCl_3$): δ (ppm) 31.03 (CH_2), 33.13 (CH_2), 33.20 (CH_2), 52.45 (CH_2), 55.15 (CH_2), 60.00 (CH_2), 119.52 (C_{quat}), 124.43 (CH), 128.96 (CH), 137.62 (C_{quat}), 168.64 (CO). IR (cm^{-1}) 3291 (νNH), 3256 (νNH), 1685 (νCO), 1597 (νCO). FAB$^+$-MS m/z ($C_{26}H_{36}N_4O_2S_3$, 532): 533 (M + H$^+$).

L^7, [15]aneS_3N_2–$CH_2CONHPh$. A solution of *N*-phenyl-2-chloroacetamide (0.295 g, 1.74 mmol) in MeCN (30 mL) was added dropwise to a rapidly stirred suspension of K_2CO_3 (0.240 g, 1.74 mmol) in MeCN (40 mL) containing [15]aneN_2S_3 (0.463 g, 0.174 mmol) which was heated at 50 °C. After the addition was complete the mixture was stirred at 50 °C overnight and the solvent was evaporated, water added and the products extracted into dichloromethane and purified by column chromatography on silica-60 (dichloromethane–methanol, 14:1 eluent) to afford 0.3 g (43%). An analytically pure sample was obtained by recrystallisation from a 1,2-dichloroethane–hexane mixture. Anal. calc. for $C_{18}H_{29}N_3OS_3$: C, 54.10; H, 7.31; N, 10.51. Found: C, 54.46; H, 7.19; N, 10.12%. ^{1}H NMR ($CDCl_3$): δ (ppm) 2.83 (m, 20H, CH_2), 3.25 (s, 2H, CH_2), 7.11 (t, 1H, Ph), 7.32 (t, 2H, Ph), 7.72 (d, 2H, Ph), 9.71 (br, s, 1H, NH). IR (cm^{-1}) 3290 (νNH), 3205 (νNH), 1669 (νCO), 1598 (νCO). FAB$^+$-MS *m*/*z* ($C_{18}H_{29}N_3OS_3$, 399): 400 ($M + H^+$).

L^8, [12]aneS_3N–$CH_2CONHPh$. Using the same procedure as outlined above for the preparation of $\mathbf{L^1}$, [12]aneNS_3 (0.133 g, 0.595 mmol) and *N*-phenyl-2-chloroacetamide (0.101 g, 0.595 mmol) afforded 0.17 g (80%) of the product as pale yellow wax after chromatography on silica-60 (dichloromethane–methanol, 40:1 eluent) and drying under reduced pressure. Anal. calc. for $C_{16}H_{24}N_2OS_3$: C, 53.89; H, 6.78; N, 7.86. Found: C, 54.00; H, 6.53; N, 7.65%. ^{1}H NMR ($CDCl_3$): δ (ppm) 2.64–2.84 (m, 16H, CH_2), 3.17 (s, 2H, CH_2), 7.07 (t, 1H, Ph), 7.30 (t, 2H, Ph), 7.67 (d, 2H, Ph), 9.41 (br, s, 1H, NH). ^{13}C NMR ($CDCl_3$): δ (ppm) 27.52 (CH_2), 28.35 (CH_2), 29.52 (CH_2), 58.66 (CH_2), 119.35 (C_{quat}), 123.96 (CH), 128.73 (CH), 137.59 (C_{quat}), 168.32 (CO). IR (cm^{-1}) 3225 (νNH), 1685 (νCO), 1601 (νCO). FAB$^+$-MS *m*/*z* ($C_{16}H_{24}N_2OS_3$, 356): 357 ($M + H^+$).

L^9, [12]aneS_2ON–$CH_2CONHPh$. Using the same procedure as outlined above for the preparation of $\mathbf{L^1}$, [12]aneNOS_2 (0.158 g, 0.762 mmol) and *N*-phenyl-2-chloroacetamide (0.129 g, 0.762 mmol) afforded 0.18 g (70%) of the product as pale yellow wax after chromatography on silica-60 (dichloromethane–methanol, 12:1 eluent) and drying under reduced pressure. Anal. calc. for $C_{16}H_{24}N_2O_2S_2$: C, 56.44; H, 7.10; N, 8.23. Found: C, 57.59; H, 7.20; N, 8.09%. ^{1}H NMR ($CDCl_3$): δ (ppm) 2.75 (m, 4H, CH_2), 2.80–2.96 (m, 8H, CH_2), 3.26 (s, 2H, CH_2), 3.78 (m, 4H, CH_2), 7.10 (t, 1H, Ph), 7.31 (t, 2H, Ph), 7.71 (d, 2H, Ph), 9.78 (br, s, 1H, NH). ^{13}C NMR ($CDCl_3$): δ (ppm) 30.68 (CH_2), 31.13 (CH_2), 53.19 (CH_2), 60.05 (CH_2), 73.61 (CH), 119.43 (C_{quat}), 123.84 (CH), 128.74 (CH), 137.92 (C_{quat}), 169.53 (CO). IR (cm^{-1}) 3220 (νNH), 1686 (νCO), 1600 (νCO). FAB$^+$-MS *m*/*z* ($C_{16}H_{24}N_2O_2S_2$, 340): 341 ($M + H^+$).

L^{10}, [12]aneS_2ON–$CH_2CONHCONH$–^{t}Bu. Using the same procedure as outlined above for the preparation of $\mathbf{L^1}$, [12]aneNOS_2 (0.33 g, 1.59 mmol) and 1-*tert*-butyl-3-(chloroacetyl)urea (0.31 g, 1.59 mmol) afforded 0.35 g (60%) of the product as a white solid. Recrystallisation by slow evaporation from methanol affords a more pure product. Anal. calc. for $C_{15}H_{29}N_3O_3S_2$: C, 49.56; H, 8.04; N, 11.56. Found: C, 47.58; H, 7.78; N, 10.55%. ^{1}H NMR ($CDCl_3$): δ (ppm) 1.37 (s, 9H, CMe_3), 2.72 (m, 4H, CH_2), 2.84 (m, 8H, CH_2), 3.76 (m, 4H, CH_2), 3.21 (s, 2H, CH_2), 8.21 (br, s, 1H, NH), 9.32 (br, s, 1H, NH). ^{13}C NMR ($CDCl_3$): δ (ppm) 28.86 (CMe_3), 29.10 (CH_2), 30.86 (CH_2), 50.69 (CMe_3), 52.58 (CH_2), 59.68 (CH_2), 74.34 (CH_2), 151.09 (CO), 172.94 (CO). IR (cm^{-1}) 3250 (νNH), 1716 (νCO), 1652 (νCO). FAB$^+$-MS *m*/*z* ($C_{15}H_{29}N_3O_3S_2$, 363): 364 ($M + H^+$).

[15]aneS_2ON_2–$(CH_2CONHCONH$–^{t}Bu)$_2$·$AgNO_3$ [$\mathbf{L^1}$·$AgNO_3$]. Anal. calc. for $C_{24}H_{46}AgN_7O_8S_2$: C, 39.34; H, 6.33; N, 13.38. Found: C, 39.35; H, 6.25; N, 13.10%. ^{1}H NMR (d^3-MeCN): δ (ppm) 1.31 (s, 18H, CMe_3), 2.71–2.96 (m, 16H, S–CH_2), 3.52 (s, 4H, CH_2), 3.65 (m, 4H, N–CH_2), 8.09 (br, s, 2H, NH), 9.45 (br, s, 2H, NH). ^{13}C NMR (d^3-MeCN): δ (ppm) 29.12 (CMe_3), 33.00 (CH_2), 35.41 (CH_2), 51.28 (CMe_3), 55.02 (CH_2), 55.21 (CH_2), 55.50 (CH_2), 68.43 (CH_2), 152.45 (CO), 173.87 (CO). IR (KBr disc, cm^{-1}) 3311 m,1715 s, 1556 s 1384 vs, 1202 s, 1110 m, 798 m, 630 m. FAB$^+$-MS *m*/*z* ($C_{24}H_{46}AgN_6O_5S_2$, 669): 669 ($\mathbf{L}Ag^+$).

[15]aneS_3N_2–$(CH_2CONHCONH$–^{t}Bu)$_2$·$AgNO_3$ [$\mathbf{L^2}$·$AgNO_3$]. Anal. calc. for $C_{24}H_{46}AgN_7O_7S_3$: C, 38.50; H, 6.19; N, 13.09. Found: C, 38.69; H, 6.07; N, 12.55%. ^{1}H NMR (d^3-MeCN): δ (ppm) 1.32 (s, 18H, CMe_3), 2.74–2.92 (m, 20H, macrocyclic CH_2), 3.38 (s, 4H, CH_2), 8.02 (br, s, 2H, NH), 8.44 (br, s, 2H, NH). IR (KBr disc, cm^{-1}) 3300 m, 1700 s, 1665 s, 1555 s, 1507 s, 1384 vs, 1255 s, 1197 m, 1100 m, 1020 m. FAB$^+$-MS *m*/*z* ($C_{24}H_{46}AgN_6O_4S_3$, 685): 685 ($\mathbf{L}Ag^+$).

[12]aneS_2ON–$CH_2CONHCONHPh$·$AgNO_3$ [$\mathbf{L^3}$·$AgNO_3$]. Anal. calc. for $C_{17}H_{25}AgN_4O_6S_2$·H_2O: C, 35.73; H, 4.76; N, 9.80. Found: C, 35.08; H, 4.33; N, 9.65%. ^{1}H NMR (d^3-MeCN): δ (ppm) 2.84 (m, 12H, S–CH_2), 3.45 (s, 2H, CH_2), 3.63 (br, s, 4H, N–CH_2), 7.12 (t, 1H, Ar), 7.35 (t, 2H, Ar), 7.49 (d, 2H, Ar), 9.04 (br, s, 1H, NH), 10.17 (br, s, 1H, NH). IR (KBr disc, cm^{-1}) 3261 m, 1718 vs, 1685 s, 1601 s, 1554 s, 1384 vs, 1324 s, 1217 s, 1116 m, 1024 m, 757 m, 695 m. FAB$^+$-MS *m*/*z* ($C_{17}H_{25}AgN_3O_3S_2$, 490): 490 ($\mathbf{L}Ag^+$).

[15]aneS_3N_2–$(CH_2CONH$–^{t}Bu)$_2$·$AgNO_3$ [$\mathbf{L^4}$·$AgNO_3$]. Anal. calc. for $C_{22}H_{44}AgN_5O_5S_3$: C, 39.87; H, 6.69; N, 10.57. Found: C, 39.46; H, 6.65; N, 10.55%. ^{1}H NMR (d^3-MeCN): δ (ppm) 1.32 (s, 18H, CMe_3), 2.67–2.91 (m, 20H, macrocyclic CH_2), 3.04 (s, 4H, CH_2), 6.58 (br, s, 2H, NH). IR (KBr disc, cm^{-1}) 3310 m, 1700 s, 1669 s, 1559 s, 1540 s, 1457 s, 1384 vs, 1327 s, 1228 s, 1120 m, 1050 m. FAB$^+$-MS *m*/*z* ($C_{22}H_{44}AgN_4O_2S_3$, 599): 599 ($\mathbf{L}Ag^+$).

[12]aneS_3N–CH_2CONH–^{t}Bu·$AgNO_3$ [$\mathbf{L^5}$·$AgNO_3$]. Anal. calc. for $C_{14}H_{28}AgN_3O_4S_3$: C, 33.20; H, 5.57; N, 8.30. Found: C, 33.20; H, 5.22; N, 8.08%. ^{1}H NMR (d^3-MeCN): δ (ppm) 1.30 (s, 9H, CMe_3), 2.87 (br, s, 16H, macrocyclic CH_2), 3.02 (s, 2H, CH_2), 6.56 (br, s, 1H, NH). IR (KBr disc, cm^{-1}) 3283 m, 1658 s, 1559 s, 1457 m, 1384 vs, 1330 s, 1265 m, 1219 m, 1110 m, 1037 w, 931 m, 905 m, 825 w. FAB$^+$-MS *m*/*z* ($C_{14}H_{28}AgN_2OS_3$, 443): 443 ($\mathbf{L}Ag^+$).

[15]aneS_3N_2–$(CH_2CONHPh)_2$·$AgNO_3$ [$\mathbf{L^6}$·$AgNO_3$]. Anal. calc. for $C_{26}H_{36}AgN_5O_5S_3$: C, 44.44; H, 5.16; N, 9.06. Found: C, 43.50; H, 5.28; N, 9.27%. ^{1}H NMR (d^3-MeCN): δ (ppm) 2.88 (m, 20H, macrocyclic CH_2), 3.39 (s, 4H, CH_2), 7.08 (t, 2H, Ar), 7.25 (t, 4H, Ar), 7.55 (d, 4H, Ar), 9.02 (br, s, 2H, NH). IR (KBr disc, cm^{-1}) 3258 m, 3133 m, 1700 s, 1676s, 1617 s, 1599 s, 1550 s, 1499 s, 1444 s, 1384 vs, 1315 s, 1249 s, 1200 s, 1104 m, 759 m, 693 m. FAB$^+$-MS *m*/*z* ($C_{26}H_{36}AgN_4O_2S_3$, 639): 639 ($\mathbf{L}Ag^+$).

[15]aneS_3N_2–$CH_2CONHPh$·$AgNO_3$ [$\mathbf{L^7}$·$AgNO_3$]. Anal. calc. for $C_{18}H_{29}AgN_4O_4S_3$·H_2O: C, 36.80; H, 5.32; N, 9.54. Found: C, 36.19; H, 4.91; N, 9.30%. ^{1}H NMR (d^3-MeCN): δ (ppm) 2.76–3.02 (m, 20H, macrocyclic CH_2), 3.44 (s, 2H, CH_2), 7.15 (t, 1H, Ar), 7.37 (t, 2H, Ar), 7.62 (d, 2H, Ar), 9.23 (br, s, 1H, NH). IR (KBr disc, cm^{-1}) 3257 m, 1685 s, 1617 s, 1597 s, 1540, 1491 s, 1444 s, 1384 vs, 1318 s, 1245 s, 1150 m, 1020 m, 761 m, 697 m. FAB$^+$-MS *m*/*z* ($C_{18}H_{29}AgN_3OS_3$, 506): 506 ($\mathbf{L}Ag^+$).

[12]aneS_3N–$CH_2CONHPh$·$AgNO_3$ [$\mathbf{L^8}$·$AgNO_3$]. Anal. calc. for $C_{16}H_{24}AgN_3O_4S_3$: C, 36.50; H, 4.60; N, 7.98. Found: C, 36.58; H, 4.47; N, 8.09%. ^{1}H NMR (d^3-MeCN): δ (ppm) 2.88 (s, 16H, macrocyclic CH_2), 3.35 (s, 2H, CH_2), 7.12 (t, 1H, Ar), 7.34 (t, 2H, Ar), 7.57 (d, 2H, Ar), 8.66 (br, s, 1H, NH). IR (KBr disc, cm^{-1}) 3290 m, 1685 s, 1597 s, 1540 s, 1497 s, 1444 s, 1384 vs,

1327 s, 1256 s, 1112 m, 1037 m, 759 m, 733 m, 697 m. FAB$^+$-MS *m*/*z* ($C_{16}H_{24}AgN_2OS_3$, 463): 463 (**L**Ag$^+$).

[12]aneS$_2$ON–CH$_2$CONHPh·AgNO$_3$ [L^9·AgNO$_3$]. Anal. calc. for $C_{16}H_{24}AgN_3O_5S_2$: C, 37.65; H, 4.74; N, 8.23. Found: C, 37.47; H, 4.61; N, 8.42%. ^{1}H NMR (d^3-MeCN): δ (ppm) 2.77–2.90 (m, 16H, macrocyclic CH_2), 3.31 (s, 2H, CH_2), 7.13 (t, 1H, Ar), 7.35 (t, 2H, Ar), 7.55 (d, 2H, Ar), 8.75 (br, s, 1H, NH). IR (KBr disc, cm^{-1}) 3290 m, 1685 s, 1664 s, 1603 s, 1551 s, 1499 s, 1449 s, 1384 vs, 1359 s, 1256 s, 1110 s, 1015 m, 762 m. FAB$^+$-MS *m*/*z* ($C_{16}H_{24}AgN_2O_2S_2$, 447): 447 (**L**Ag$^+$).

Acknowledgements

We thank the EPSRC, The University of Nottingham, the EPSRC National Mass Spectrometry Service at the University of Swansea and the EPSRC National Service for Crystallography at the University of Southampton.

References and notes

1 (*a*) S. R. Cooper, *Acc. Chem. Res.*, 1988, **21**, 141; (*b*) A. J. Blake and M. Schröder, *Adv. Inorg. Chem.*, 1990, **35**, 1; (*c*) S. C. Rawle and S. R. Cooper, *Struct. Bonding (Berlin)*, 1990, **72**, 1.

2 T. Adachi, M. D. Durrant, D. L. Hughes, C. J. Pickett, R. L. Richards, J. Talarmin and T. Yoshiba, *J. Chem. Soc., Chem. Commun.*, 1992, 1464; A. J. Blake, A. Taylor and M. Schröder, *Polyhedron*, 1990, **9**, 2911; A. J. Blake, R. O. Gould, A. J. Holder, A. J. Lavery and M. Schröder, *Polyhedron*, 1990, **9**, 2919; A. J. Blake, M. A. Halcrow and M. Schröder, *J. Chem. Soc., Dalton Trans.*, 1994, 1631 and refs. cited therein; C. Landgrafe and W. S. Sheldrick, *J. Chem. Soc., Dalton Trans.*, 1996, 989; K. Brandt and W. S. Sheldrick, *J. Chem. Soc., Dalton Trans.*, 1996, 1237; A. J. Blake, D. W. Bruce, I. A. Fallis, S. Parsons, H. Richtzenhain, S. A. Ross and M. Schröder, *Philos. Trans. R. Soc. London, Ser. A*, 1996, **354**, 395; R. D. Adams, S. B. Fallon, J. L. Perrin, J. A. Queisser and J. H. Yamamoto, *Chem. Ber.*, 1996, **129**, 313 and refs. cited therein; G. J. Grant, K. E. Rogers, W. N. Setzer and D. G. Van Derveer, *Inorg. Chim. Acta*, 1995, **234**, 35; H.-J. Kim, J.-H. Lee, I.-H. Suh and Y. Do, *Inorg. Chem.*, 1995, **34**, 796; M. Munakata, L. P. Wu, M. Yamamoto, T. Kuroda-Sowa and M. Maekawa, *J. Chem. Soc., Dalton Trans.*, 1995, 3215.

3 A. J. Blake, A. J. Holder, T. I. Hyde and M. Schröder, *J. Chem. Soc., Chem. Commun.*, 1987, 987; A. J. Blake, R. O. Gould, J. A. Greig, A. J. Holder, T. I. Hyde, A. J. Lavery, M. O. Odulate and M. Schröder, *J. Chem. Soc., Chem. Commun.*, 1987, 118; S. C. Rawle, R. Yagbasan and S. R. Cooper, *J. Am. Chem. Soc.*, 1987, **109**, 6181; A. J. Blake, R. O. Gould, A. J. Holder, T. I. Hyde and M. Schröder, *J. Chem. Soc., Dalton Trans.*, 1988, 1681; A. J. Blake, R. O. Gould, J. A. Greig, A. J. Holder, T. I. Hyde and M. Schröder, *J. Chem. Soc., Chem. Commun.*, 1989, 876; A. J. Blake, R. O. Gould, J. A. Greig, A. J. Holder, T. I. Hyde, A. Taylor and M. Schröder, *Angew. Chem., Int. Ed. Engl.*, 1990, **29**, 197; A. J. Blake, A. J. Holder, T. I. Hyde, G. Reid and M. Schröder, *Polyhedron*, 1989, **8**, 2041; W. N. Setzer, Q. Guo, G. J. Grant, J. L. Hubbard, R. L. Glass and D. G. VanDerveer, *Heteroat. Chem.*, 1990, **1**, 317; T. E. Jones, L. S. W. L. Sokol, D. B. Rorobacher and M. D. Glick, *J. Chem. Soc., Chem. Commun.*, 1979, 140.

4 D. S. L. Fekete and H. Meider, *J. Inorg. Nucl. Chem.*, 1980, **42**, 885; D. Sevdic and H. Meider, *J. Inorg. Nucl. Chem.*, 1981, **43**, 153; E. Sekido, H. Kawahara and K. Tsuji, *Bull. Chem. Soc. Jpn.*, 1988, **61**, 1587; H. Takeshita, A. Mori and S. Hirayama, *J. Chem. Soc., Chem. Commun.*, 1989, 564.

5 A. J. Blake, J. P. Danks, I. A. Fallis, A. Harrison, W.-S. Li, S. Parsons, S. A. Ross, G. Whittaker and M. Schröder, *J. Chem. Soc., Dalton Trans.*, 1998, 3969 and refs. cited therein.

6 V. V. Pavlishchuk and P. E. Strizhak, *Chem. Heterocycl. Compd.*, 1989, **25**, 553; L. G. A. van de Water, F. ten Hoonte, W. L. Driessen, J. Reedijk and D. C. Sherrington, *Inorg. Chim. Acta*, 2000, **303**, 77.

7 L. Siegfried and T. A. Kaden, *Helv. Chim. Acta*, 1984, **67**, 29.

8 D. St. C. Black and I. A. McLean, *Aust. J. Chem.*, 1971, **24**, 1401; D. St. C. Black and I. A. McLean, *Tetrahedron Lett.*, 1969, **45**, 3961; S. Shinkai, K. Shigematsu, Y. Honda and O. Manabe, *Bull. Chem. Soc. Jpn.*, 1984, **57**, 2879; D. Pelissard and R. Louis, *Tetrahedron Lett.*, 1972, **45**, 4589; J. Jurczak, S. Kasprzyk, P. Salanski and T. Stankiewicz, *J. Chem. Soc., Chem. Commun.*, 1991, 956; D. Baldwin, P. A. Duckworth, G. R. Erickson, L. F. Lindoy, M. McPartlin, G. M. Mockler, W. E. Moody and P. E. Tasker, *Aust. J. Chem.*, 1987, **40**, 1861; Z. Yang, J. S. Bradshaw, X. X. Zhang, P. B. Savage, K. E. Krakowiak, N. K. Dalley, N. Su, R. T. Bronson and R. M. Izatt, *J. Org. Chem.*, 1999, **64**, 3162; R. T. Bronson, J. S. Bradshaw, P. B. Savage, S. Fuangswasdi, S. C. Lee, K. E. Krakowiak and R. M. Izatt, *J. Org. Chem.*, 2001, **66**, 4752; M. Tanaka, M. Nakamura, T. Ikeda, K. Ikeda, H. Ando, Y. Shibutani, S. Yajima and K. Kimura, *J. Org. Chem.*, 2001, **66**, 7008.

9 L. R. Hoover, T. Pryor, J. A. Wetgenant, P. E. Williams, B. N. Storhoff and J. C. Huffman, *Phosphorus, Sulfur Silicon Relat. Elem.*, 1997, **122**, 155; J. Ishikawa, H. Sakamoto, M. Nakamura, K. Doi and H. Wada, *J. Chem. Soc., Dalton Trans.*, 1999, 191; R. C. Liu, P.-S. Fung, F. Xue, T. C. W. Mak and D. K. P. Ng, *J. Chem. Res., Synop.*, 1998, **8**, 1744; H. Sakamoto, J. Ishikawa and M. Otomo, *Bull. Chem. Soc. Jpn.*, 1995, **68**, 2631; R. C. W. Liu, P.-S. Fung, F. Xue, T. C. W. Mak and D. K. P. Ng, *J. Chem. Res. (S)*, 1998, 414.

10 (*a*) M. M. G. Antonisse and D. N. Reinhoudt, *Chem. Commun.*, 1998, 443; (*b*) P. D. Beer, P. K. Hopkins and J. D. McKinney, *Chem. Commun.*, 1999, 1253; (*c*) J. B. Cooper, M. G. B. Drew and P. D. Beer, *J. Chem. Soc., Dalton Trans.*, 2001, 392.

11 J. E. Redman, P. D. Beer, S. W. Dent and M. G. B. Drew, *Chem. Commun.*, 1998, 231; P. D. Beer and S. W. Dent, *Chem. Commun.*, 1998, 825.

12 D. M. Rudkevich, Z. Brzozka, M. Palys, H. C. Visser, W. Verboom and D. N. Reinhoudt, *Angew. Chem., Int. Ed. Engl.*, 1994, **33**, 467; D. M. Rudkevich, J. D. Mercer-Chalmers, W. Verboom, R. Ungaro, F. de Jong and D. N. Reinhoudt, *J. Am. Chem. Soc.*, 1995, **117**, 6124.

13 E. A. Arafa, K. I. Kinnear and J. C. Lockhart, *J. Chem. Soc., Chem. Commun.*, 1992, 61.

14 M. T. Reetz, C. M. Niemeyer and K. Harms, *Angew. Chem.*, 1991, **103**, 1515; M. T. Reetz, C. M. Niemeyer and K. Harms, *Angew. Chem., Int. Ed. Engl.*, 1991, **30**, 1472; M. T. Reetz, C. M. Niemeyer and K. Harms, *Angew. Chem., Int. Ed. Engl.*, 1991, **30**, 1474.

15 D. M. Rudkevich, A. N. Shivanayuk, Z. Brzozka, W. Verboom and D. N. Reinhoudt, *Angew. Chem., Int. Ed. Engl.*, 1995, **34**, 2124.

16 H. A. Miller, N. Laing, S. Parsons, A. Parkin, P. A. Tasker and D. J. White, *J. Chem. Soc., Dalton Trans.*, 2000, 3773; D. J. White, N. Laing, H. Miller, S. Parsons, S. Coles and P. A. Tasker, *Chem. Commun.*, 1999, 2077.

17 J. B. Love, J. M. Vere, M. W. Glenny, A. J. Blake and M. Schröder, *Chem. Commun.*, 2001, 2678.

18 J. Scheerder, R. H. Vreekamp, J. F. J. Engbersen, W. Verboom, J. P. M. van Duynhoven and D. N. Reinhoudt, *J. Org. Chem.*, 1996, **64**, 3476.

19 K. A. Connors, *Binding Constants*, John Wiley and Sons, New York, 1987, 24.

20 (*a*) T. R. Kelly and M. H. Kim, *J. Am. Chem. Soc.*, 1994, **116**, 7072; (*b*) P. D. Beer and P. A. Gale, *Angew. Chem., Int. Ed.*, 2001, **40**, 486 and refs. cited therein.

21 Benzoates are well known to bind strongly to ureas in apolar solvents, and appreciable binding (150 M^{-1}) is observed in DMSO; see ref. 20*a*.

22 J. M. Alia and H. G. M. Edwards, *J. Solution Chem.*, 2000, **29**, 781; Y. Pocker and D. N. Kevill, *J. Am. Chem. Soc.*, 1965, **87**, 4760.

23 For some examples, see: H. Keijiang, J. S. Bradshaw, V. N. Pastushok, K. E. Krakowiak, N. K. Dalley, X. X. Zhang and R. M. Izatt, *J. Org. Chem.*, 1998, **63**, 4786; J. A. R. Navarro, M. A. Romero, J. M. Salas, R. Faure and X. Solans, *J. Chem. Soc., Dalton Trans.*, 1997, 2321; J. J. H. Edema, H. T. Stock, J. Buter, R. M. Kellogg, W. J. J. Smeets, A. L. Spek and F. van Bolhuis, *Angew. Chem., Int. Ed. Engl.*, 1993, **32**, 436; J. Perron and A. L. Beauchamp, *Can. J. Chem.*, 1984, **62**, 1287.

24 The Cambridge Structural Database, Version 5.21, April 2001. The mean Ag–O distance found for this type of compound is 2.48 Å.

25 The mean Ag–S distance for thioether macrocyclic compounds found in the Cambridge Structural Database, Version 5.21, April 2001, is 2.62 Å. Some representative examples of thioether crown Ag$^+$ complexes with 4-, 5- and 6-co-ordination are: U. Kallert and R. Mattes, *Inorg. Chim. Acta*, 1991, **180**, 263; R. Louis, Y. Agnus and R. Weiss, *Acta Crystallogr., Sect. B*, 1977, **33**, 1418; A. J. Blake, R. O. Gould, W.-S. Li, V. Lippolis, S. Parsons, C. Radek and M. Schröder, *Inorg. Chem.*, 1998, **37**, 5070; A. J. Blake, D. Collison, R. O. Gould, G. Reid and M. Schröder, *J. Chem. Soc., Dalton Trans.*, 1993, 521.

26 A. J. Blake, R. O. Gould, G. Reid and M. Schröder, *J. Chem. Soc., Chem. Commun.*, 1990, 974; A. J. Blake, G. Reid and M. Schröder, *J. Chem. Soc., Chem. Commun.*, 1992, 1074; A. J. Blake, R. O.

Gould, C. Radek and M. Schröder, *J. Chem. Soc., Chem. Commun.*, 1994, 985.
27 M. Munakata, M. Wen, Y. Suenaga, T. Kuroda-Sowa, M. Maekawa and M. Anahata, *Polyhedron*, 2001, **20**, 2037.
28 M. J. Hynes, *J. Chem. Soc., Dalton Trans.*, 1993, 311.
29 R. Herges, A. Dikmans, U. Jana, F. Kohler, P. G. Jones, I. Dix, T. Fricke and B. Konig, *Eur. J. Org. Chem.*, 2002, **17**, 3004.
30 M. Albrecht, J. Zauner, R. Burgert, H. Rottele and R. Frohlich, *Mater. Sci. Eng., C: Biomimetic and Supramolecular Systems*, 2001, **18**, 185.
31 M. G. B. Drew, *Prog. Inorg. Chem.*, 1977, **23**, 67.
32 D. L. Kepert, *Prog. Inorg. Chem.*, 1979, **25**, 41.
33 L. Dupont, L. Lewinski, K. Stadnicka and J. Delarge, *Cryst. Struct. Commun.*, 1981, **10**, 925; L. Dupont, O. Dideberg, J. Delarge, G. Dive and L. Thunus, *Acta Crystallogr., Sect. B*, 1982, **38**, 1495; V. Velikova, S. Bakardjeva and O. Angelova, *Acta Crystallogr., Sect. C*, 1999, **55**, 1328; L. Dupont, O. Dideberg, B. Masreel, J. Delarge, M. Schynts and B. Pirotte, *Acta Crystallogr., Sect. C*, 1991, **47**, 2152; S. Harkema and D. Feil, *Acta Crystallogr., Sect. B*, 1969, **25**, 589.
34 J. Cosier and A. M. Glazer, *J. Appl. Crystallogr.*, 1986, **19**, 105.
35 G. M. Sheldrick, SHELXS-97, University of Göttingen, Germany, 1997.
36 G. M. Sheldrick, SHELXL-97, University of Göttingen, Germany, 1997.